Title

Broadband energy harvesting via adaptive control of bistable potential energy separatrix

ISBN

9780819499837

Authors

Ouellette, Scott A

Todd, Michael D

Publication Date

2014-03-09

DOI

10.1117/12.2044866

Peer reviewed

Broadband Energy Harvesting via Adaptive Control of Bistable Potential Energy Separatrix

Scott A. Ouellette, Michael D. Todd
University of California, San Diego, 9500 Gilman Dr. MC-0085, La Jolla, CA, 92093-0085

ABSTRACT

As a result of the documented performance limitations of conventional linear piezoelectric energy harvesters, researchers have focused their efforts towards device designs that can better capture broadband energy. The approaches used can be classified into three categories: frequency tuning, multi-modal energy harvesting, and nonlinear energy harvesting[1]. Of the nonlinear harvesting approaches studied, bistable energy harvesters have been shown to have the most robust performance when subjected to broadband harmonic & stochastic excitation[2-4]. A conventional method for developing a nonlinear bistable restoring force is through use of magnetic repulsion. In these studies, a common theme of high-energy orbit breakdown occurs during a frequency upsweep. The issue at hand is the inability of the device inertial forces to overcome the potential energy barrier (separatrix) inherent to a bistable potential energy.

This paper proposes the use of a high-permeability electromagnet for adaptively controlling the bistable magnetic repulsion force to expand the frequency bandwidth for high-energy harmonic oscillations. Numerical simulations of the nonlinear oscillator are used to study the system response under varying parameters of separation distance and electromagnetic coil current. An analytical model of the magnetic moment of an electromagnet is developed for use in studying the force interaction between repulsing magnets and to determine the parametric space that generates buckling loads in a cantilever bimorph energy harvester.

Keywords: Energy Harvesting, Bistable Dynamics, Electromagnetics

1. INTRODUCTION

Piezoelectric inertial generators have been a significant research focus for vibration-based energy harvesting platforms since the early 2000s. The conventional design studied is that of a cantilever beam with a tip mass and a bimorph piezoelectric configuration. Maximum power generation occurs when the beam is excited at the primary resonance frequency, and, as such, the design protocol requires an analysis of the excitation spectrum in order to determine the appropriate parameters like beam dimensions and tip mass[5-7]. This type of configuration is conventionally categorized as a linear, narrow-band vibration energy harvester. For clarification, in this paper the classification between a linear and nonlinear energy harvester relates to the potential energy of the restoring force (i.e. beam stiffness). While this approach is relatively simple to adopt, the fact remains that most vibration excitation sources have an inherent frequency spectrum, and that designing an energy harvester to match a single frequency is highly inefficient. As such, the focus of vibration energy harvesting has shifted towards broadband techniques / designs[8–14].

Erturk and Elvin[1] compiled the many research articles and classified the broadband approaches into three categories: frequency tuning, multi-modal energy harvesting, and nonlinear energy harvesting. While each technique has its advantages, this paper will focus on the use of a nonlinear restoring force to generate a broadband resonant condition. Within the class of nonlinear energy harvesting, there are three noted manifestations: monostable, bistable, and bi-linear/piecewise linear. Again, while there are characteristics unique to each type of nonlinear condition, the general consensus amongst researchers is that the bistable approach is the most robust with respect to broadband energy transduction.

Bistable energy harvesters exhibit a unique set of response oscillation solutions that can result from the input excitation. When dealing with nonlinear oscillations, the system response is a function of the input energy, which accounts for both the excitation frequency and amplitude. For bistable oscillators, the three response types, ordered from high energy to low, are: interwell, chaotic, and intrawell[2]. What makes the bistable configuration an attractive approach is that the interwell (high-energy) orbits exist over a fairly broad frequency spectrum[11]. Additionally, bistable energy harvesters have been demonstrated to exhibit a unique condition referred to as stochastic resonance in which the device has an interwell response when subjected to a Gaussian random process[4].

While bistable configurations have been demonstrated to exhibit many favorable characteristics, there still exists a set of low-energy responses resulting from the competing inertial forces of the tip mass and the bistable well separatrix. For many bistable energy harvesters, the double-well restoring potential is generated by means of magnetic repulsion[11]. Other approaches used in developing a bistable potential have been via a compressed buckled beam[3],[15], and magnetic attraction[16]; however, these methods are not of particular interest to this study. This paper presents a novel approach to the control of a bistable potential well generated by repulsing magnets. Specifically, the approach employs the use of a high-permeability electromagnet to perturb the magnetic field generating the bistable potential well, as shown below in Figure 1.

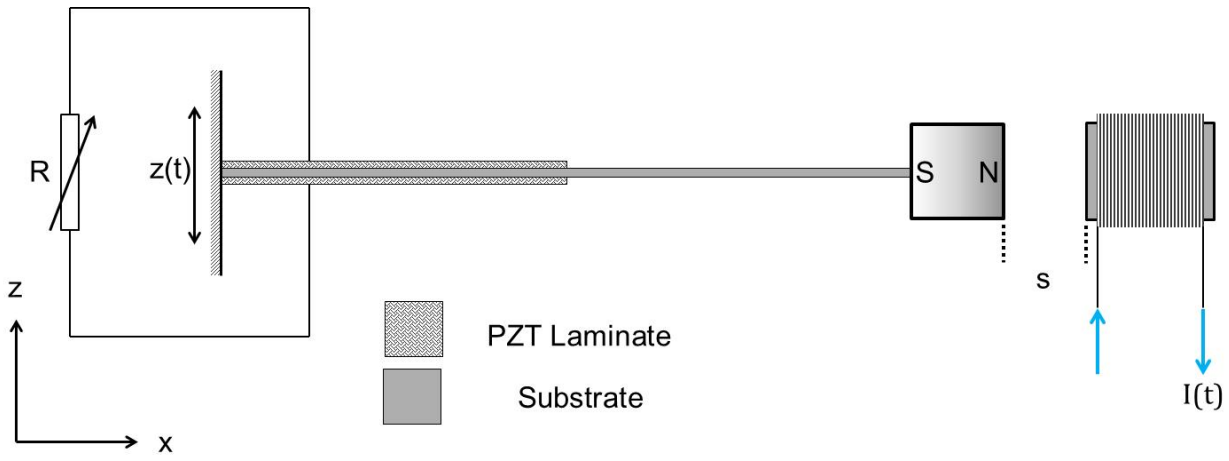

Figure 1: Proposed broadband energy harvester setup using a high permeability electromagnet.

The following sections of this paper will present an analytical model of the interaction between repulsing magnets, a derivation for a simple iron-cored solenoid (electromagnet), and a parametric study of the specific terminal parameters that dictate the magnetic field. This study is to investigate the power demands required by the electromagnet to properly control the bistable separatrix in a manner that increases the broadband interwell resonance response. Ultimately, an electromagnet design that generates a net-positive power output for the expanded interwell response frequency spectrum is the primary goal. A review of previous attempts in perturbation methods and frequency tuning for vibration energy harvesters is presented below for reference.

2. PREVIOUS STUDIES IN ADAPTIVE BOUNDARY CONDITIONS

In attempts to achieve broadband resonance, researchers have investigated several tuning methods to increase the resonance bandwidth of vibration-based energy harvesters. Erturk and Elvin[1] classify the tuning methods as either manual tuning (i.e. operator intervention required) and self-tuning. While manual tuning is technically a low-power solution, its implementation is sub-optimal due to the necessity of human intervention. Self-tuning methods, by comparison, are much more attractive for remote energy harvesting applications as the device could potentially

provide autonomous power to a sensor node (or system) well beyond the functional lifetime of a conventional battery. An essential criterion for self-tuning methods to be feasible for vibration energy harvester designs is that they generate a net-positive power output.

The first reported self-tuning energy harvesters used magnetic boundary conditions to alter the restoring potential of a cantilever beam inertial generator[17],[18]. The approach outlined by Zhu et al.[17] used a linear actuator to control the separation distance between two attracting magnets – keeping in mind that magnetic attraction configurations result in a monostable potential. The device featured a microcontroller that would periodically measure the output voltage of the energy harvester and then drive the linear actuator as needed. The microcontroller instructions were defined by comparing the voltage to a threshold condition to ensure resonance; however, that approach was shown to suffer from detection inefficiencies. Subsequently, an improved resonance detection method was proposed by Ayala-Garcia et al.[18] which exploited the phase difference between the harvester and base to set the resonance threshold condition. While these papers proposed the designs as self-tuning, the power used for driving the linear actuator was not derived from the vibration energy capture. Studies were performed to determine the amount of time required to store enough charge in a supercapacitor for a tuning process, and the results showed an average charge time of 2 hours required for a single tuning – an insufficient result for environments with highly non-stationary excitation sources.

The concept proposed in this paper is to manipulate the bistable potential separatrix by adaptively changing the current direction within an iron-cored solenoid (i.e. an electromagnet). By altering the coil current direction, the potential energy of the system restoring force can transition between monostable and bistable, as shown below in Figure 2.

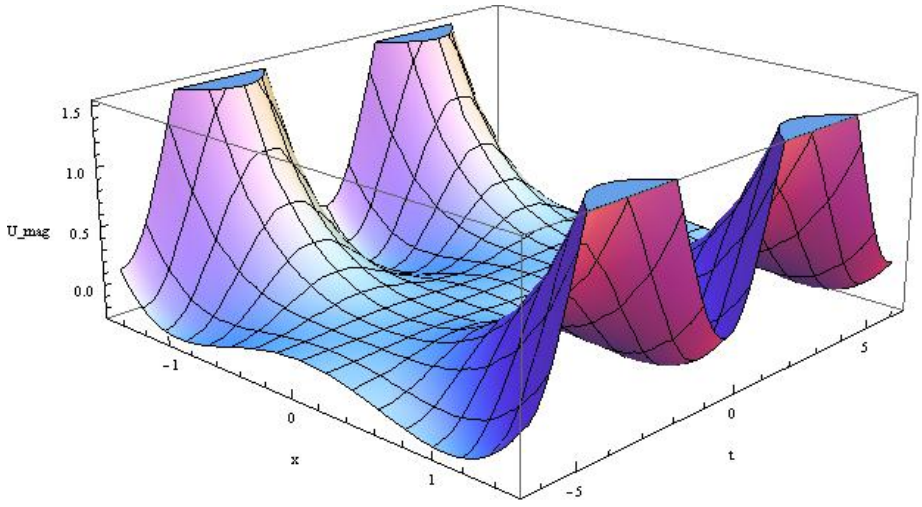

Figure 2: A 3-dimensional non-stationary potential well representing a disappearing /oscillating bistable separatrix.

3. REPULSING MAGNETIC INTERACTION MODEL

In order to define the essential parameters of the electromagnet, it is first important to understand the repulsing interaction, and how it is used to generate a bistable potential. An analytical study of the force between repulsing magnets was developed by Landecker et al.[19], and is the basis for this section. Stanton et al.[11] expanded on the analysis provided by Landecker to show how the resulting magnetic potential generates a bistable potential in a cantilever inertial generator. The important aspects of these studies are presented here to highlight the salient properties required in the analysis of the electromagnet.

In essence, a variational approach to determining the magnetic potential between repulsing magnets was shown to be a function of the respective magnetic moments (μ) and their separation distance (**r**), as described in equations (1) and (2). Please note the bold **r** denotes a vector expression, $\| \circ \|_2$ denotes a Euclidean norm, and that ∇ is the vector gradient with respect to the Cartesian basis. A system diagram is shown below in Figure 3, and the resulting magnetic potential as a function of vertical displacement (α) and rotation (θ) is shown in Figure 4.

$$\vec{B}_{p-em} = -\frac{\mu_0}{4\pi}\nabla\frac{\overrightarrow{\mu_p}\cdot\vec{r}}{\|\vec{r}\|_2^3} \tag{1}$$

$$U_m = \vec{B}_{p-em}\cdot\vec{\mu}_{em}(t) \tag{2}$$

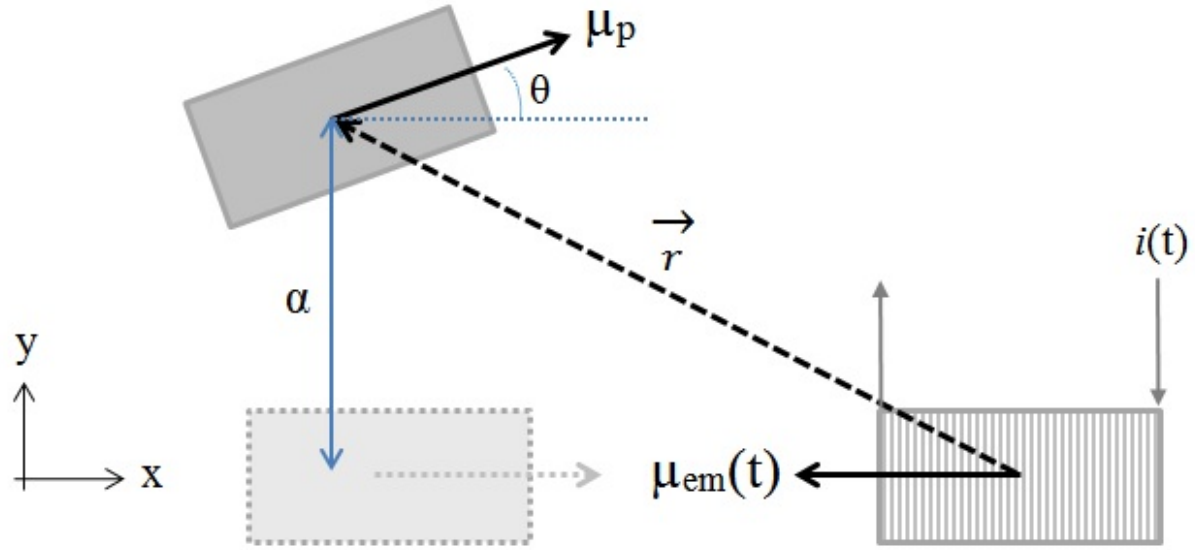

Figure 3: A representative magnetic repulsion diagram derived from Landecker et al.[19]

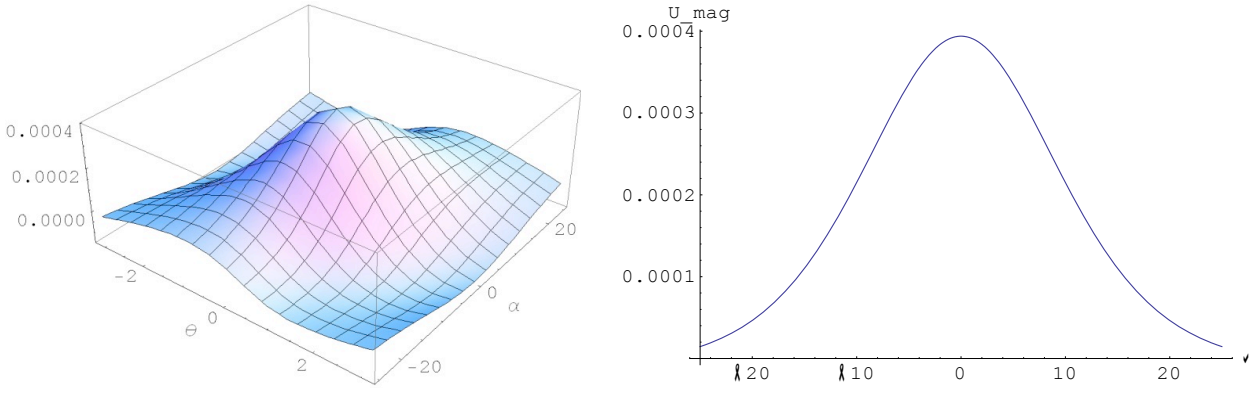

Figure 4: The magnetic potential energy generated by two repulsing magnets for various vertical and rotational values. The image on the right depicts the condition in which the magnetic moment vectors are perfectly aligned.

As shown by equations (1) and (2), the magnitude of the magnetic potential (U_m) is highly related to the magnitude of the magnetic moments. An expression for the magnetic moment of a magnet (e.g. a neodymium bar magnet) asserts the leading order behavior relates to the magnetization vector (**M**) and the magnet volume (V). For a permanent magnet, the magnetization vector can be approximated using the residual flux density (B_r), where $M = B_r/\mu_0$. For an electromagnet, however, an approximate expression for the magnetic moment is much more complicated. The following section will focus on reviewing the necessary concepts with which to analyze the magnetic field of an electromagnet.

4. ELECTROMAGNET MODEL & POWER ANALYSIS

In order to derive an approximate equation for the magnetic moment produced by an electromagnet, it is first necessary to review the properties of a solenoid (i.e. an electromagnet without an iron core). In essence, a solenoid is a wire coil that generates a magnetic field when an electric current is applied. The magnetic field is conventionally described by two parameters, the magnetic flux density (**B**-field), and the magnetic field strength (**H**-field). These two fields relate to the electric terminal as follows:

An important conventional note for clarity is that magnetic permeability (μ) is not the same as the magnetic moment (**μ**). For a solenoid, the core is made of air, and thus the two fields are related by the permeability of free space ($\mu_0 = 4\pi \times 10^{-7}$ [N/A^2]). While the permeability for an iron core is much higher allowing for a large **B**-field with little current, the relationship between the two fields is highly nonlinear – an issue that will be addressed later on in this paper.

In this study, all of the magnets will be cylindrical in geometry, thus necessitating the use of cylindrical coordinates when deriving the **B**-field for a solenoid. For an ideal solenoid consisting of a single coil layer that is tightly packed, and infinitely long, the axial (z-direction) component of the B-field is simply:

$$B_z = \mu_0 nI \tag{3}$$

While the field expression becomes much more complicated for a finite length solenoid, there have been several studies that develop closed-form solutions of the respective **B**-fields[20–22]. Most recently, Derby and Olbert[22] presented a solution which makes use of the cylindrical symmetry to implement a special case of a generalized complete elliptic integral for determining the radial (ρ) and axial (z) B-field components. Equations 4a-b below are used to describe the axial component of a finite solenoid of radius (a) and length (2b).

$$C(k_c, p, c, s) = \int_0^{\pi/2} \frac{(c\ cos^2\varphi + s\ sin^2\varphi)d\varphi}{(cos^2\varphi + p\ sin^2\varphi)\sqrt{cos^2\varphi + k_c^2 sin^2\varphi}} \tag{4a}$$

$$B_z = \frac{\mu_0 nIa}{\pi(a+\rho)}[\beta_+ C(k_+, \gamma^2, 1, \gamma) - \beta_- C(\beta_-, \gamma^2, 1, \gamma)] \tag{4b}$$

Note, the constants ($\beta_\pm$, $k_\pm$, and γ) are all geometric constants based on the cylinder dimensions. The authors provide a sample code for quickly evaluating the complete elliptic integral, and while this approach is fairly accurate, the equations break-down at the solenoid boundaries ($\rho = a$, and $z = \pm b$).

The addition of an iron core to the solenoid has two notable effects: 1) the magnetic field generated per unit of coil current increases greatly due to the alignment of magnetic domains within the core, making special note that the relative permeability of soft iron cores is in the range of 10^3-10^5, and 2) the field direction is focused within the boundary of the core. Unlike air, an iron core has a finite set of magnetic domains, and thus will saturate. When the magnetizing current is reduced to zero, the iron core still remains magnetized, and thus the material exhibits a hysteretic relationship between the two fields, as shown below in Figure 5a. It is important to note that once a magnetizing field is applied to the core, it will only return to a de-magnetized state if it is heated to its Curie temperature. For this study, the core characteristics are idealized such that the relationship is piecewise linear, as shown in Figure 5b.

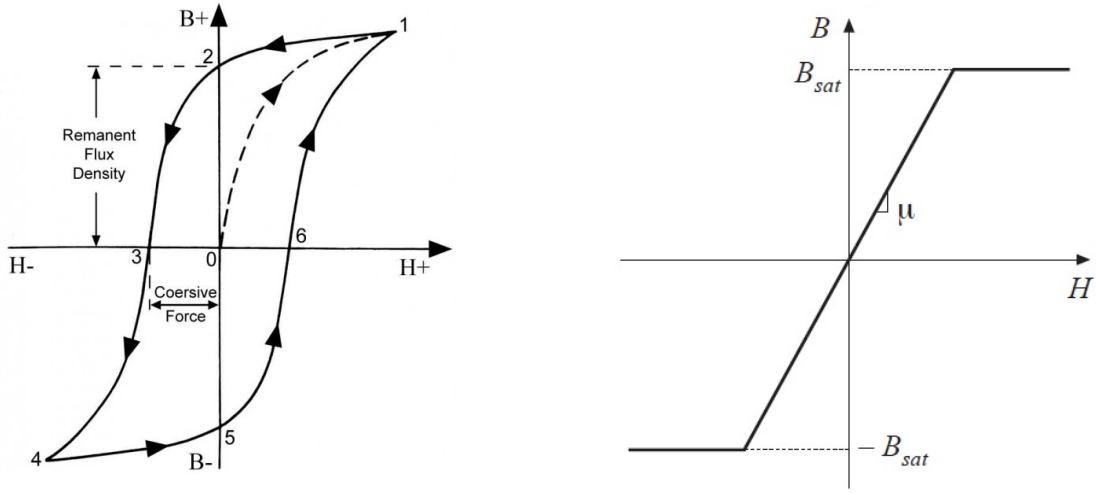

Figure 5: (a) characteristic curve tracing for iron core. At point 0 the material is un-magnetized. Once a magnetizing field is applied, typically via a current carrying coil, the magnetic domains align and the **B**-field saturates at point 1. Once the coil current is reduced to zero, the magnetism in the material domains remain. (b) An idealized, no-loss, core representation used for simple analyses.

Now that a basic foundation for the electromagnet behavior is established, this paper will focus on deriving an approximate expression for the magnetic moment generated by a cylindrical electromagnet, as depicted below in Figure 6a. To start, this study will assume the magnetization vector, **M**, will be of similar form to the permanent magnet. The restricting condition is that the electromagnet will behave like a permanent magnet when the core is saturated. Thus, the following condition is considered:

$$\boldsymbol{M} = \frac{B_{sat}}{\mu_0} \tag{5}$$

To do this, we must first establish principles of magnetic circuits to account for the effect of the open loop. A fundamental principle of electromagnet analysis is that the magnetic field forms a closed loop from one pole to the other. For a simple toroidal inductor, the path is completed by the core, and thus the field strength, **H**(t), can be assumed to be uniform. The magnetomotive force (MMF), $\mathcal{F}$(t), between two points, x_1 and x_2, is simply the

integral of the **H**-field between the points. Thus, for a uniform **H**-field, the MMF is: $\mathcal{F} = H\ell$, where ℓ is the distance between points. Additionally, the total magnetic flux, $\phi(t)$, is the sum of all flux density vectors through a surface, A_c. Therefore, a uniform flux density through a surface with area, A_c, yields the expression: $\phi(t) = \mathbf{B}A_c$.

Simple application of Ampere's Law to a closed loop inductor – very similar to an electromagnet – shows the MMF is equivalent to the total current in the coil (i.e. $\mathcal{F} = H\ell = ni(t)$). Assuming the applied current is such that the (idealized) core is saturated, then the following expression holds:

$$I_{sat} = \frac{B_{sat} l_m}{\mu n} \tag{6}$$

Solving equation (6) for the saturation magnetic field, the following expression for the magnetic moment of a closed loop electromagnet as a function of the total current is generated:

$$\vec{\mu}_{em} = \frac{I_{sat}\mu n}{l_m \mu_0} V_{em} \tag{7}$$

It is important to further note that the saturation **B**-field for a soft-magnetic iron core is usually known or provided by the material supplier. While the expression in equation (7) is nice, it does not account for the effect of the air gap on the saturation current. To account for this effect, a simple magnetic circuit model is used. The essential assumptions for a magnetic circuit using an analog of Kirchhoff's node laws are as follows:

- The divergence of **B** = 0;
- Flux lines are continuous with no end;
- Total flux entering a node must be zero;
- The magnetic force and flux are uniform through an element with cross-sectional surface area, A_c (added for completeness)

(a) **(b)**

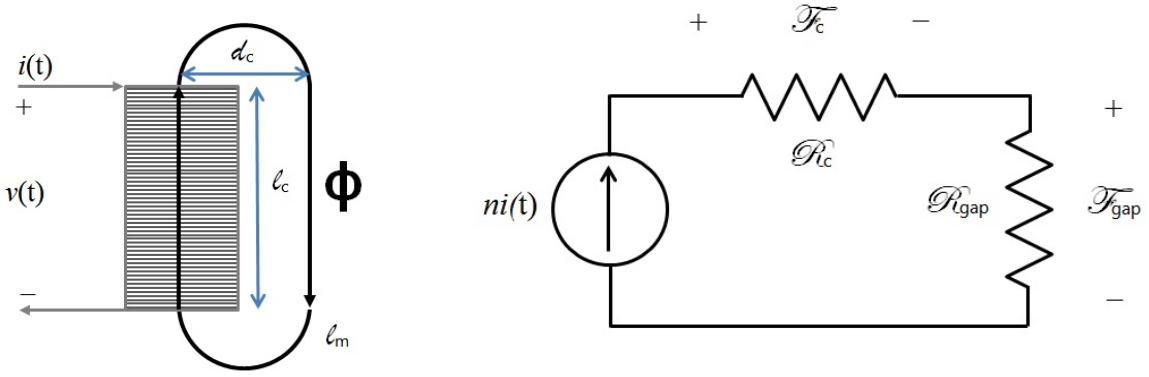

Figure 6: (a) diagram of a cylindrical electromagnet with an assumed magnetic field path (ϕ) shown. (b) an equivalent magnetic circuit accounting for the air gap reluctance, $\mathcal{R}_{gap}$.

Based on those assumptions, the application of Ampere's Law to the magnetomotive force places a restriction that the **H**-field is evaluated over a closed path. Applying the rules listed above to the system shown in Figure 6b, the following expression for Ampere's Law is derived:

$$ni = \phi(R_c + R_{gap}) \tag{8a}$$

$$R_c = \frac{l_c}{\mu A_c} \tag{8b}$$

$$R_{gap} = \frac{l_{gap}}{\mu_0 A_c} = \frac{l_c + \pi d_c}{\mu_0 A_c} \tag{8c}$$

Please note, the magnetic path length was calculated as from the center of the iron core and assumes a semi-circular rotation with a diameter equivalent to the core diameter. Applying equations (8a-c) to equation (5), and assuming a cylindrical electromagnet with an ideal iron core, yields the following expression for the magnetic moment:

$$\vec{\mu}_{em} = \frac{n\pi r_c^2 h_c}{\mu_0 A_c \left(\frac{l_c}{\mu A_c} + \frac{l_c + \pi d_c}{\mu_0 A_c}\right)} \begin{cases} i(t) \;\; for \; |H| < {}^{B_{sat}}/_{\mu} \\ I_{sat} \;\; for \; H \geq {}^{B_{sat}}/_{\mu} \end{cases} \tag{9}$$

A cursory analysis of equation (9) shows the large effect on the air gap significantly increases the saturation current. As such, the required number of coil turns, n, increases greatly to offset the air gap reluctance. However, there are two issues associated with increasing the number of coil turns that lead to diminishing returns: 1) for a finite cylinder height, h_c, the increasing number of turns will require coil overlap which results in increased coil diameter, and 2) the increased coil length adds to the parasitic resistance, which thus requires a higher terminal voltage, and higher DC power loss due to joule heating.

5. CONCLUSIONS

The focus of this initiative is the use of a high permeability electromagnet to adaptively control the bistable separatrix of a piezoelectric inertial generator for broadband vibration energy harvesting. This paper analytically investigated the properties of an iron-cored solenoid in order to develop an approximate expression for the magnetic moment generated for a given coil current. To demonstrate the feasibility of the concept, the paper detailed several published articles to set a basis for further research. The preliminary analysis of the physics involved shows many hurdles that need addressing prior to implementation. Namely, in order for the proposed system to be effective, it must have a net-positive power output. Since the electromagnet requires a constant applied current to generate a strong enough magnetic field, the feasibility is already suspect. However, current research is underway in hybrid magnetic-repulsion boundary condition systems that would utilized an electromagnet in a pulsed operation to perturb the bistable separatrix such that a high-energy interwell oscillation is induced for excitation frequencies beyond the current range reported.

REFERENCES

[1] Elvin, N., and Erturk, A., [Advances in energy harvesting methods] , Springer (2013).

[2] Harne, R.L., and Wang, K.W., "A review of the recent research on vibration energy harvesting via bistable systems," Smart Materials and Structures 22(2), 023001 (2013).

[3] Zhu, Y., and Zu, J.W., "Enhanced buckled-beam piezoelectric energy harvesting using midpoint magnetic force," Applied Physics Letters 103(4), 041905–041905 (2013).

[4] Cottone, F., Vocca, H., and Gammaitoni, L., "Nonlinear Energy Harvesting," Physical Review Letters 102(8), 080601 (2009).

[5] Erturk, A., and Inman, D.J., "Issues in mathematical modeling of piezoelectric energy harvesters," Smart Materials and Structures 17(6), 065016 (2008).

[6] Erturk, A., and Inman, D.J., "A Distributed Parameter Electromechanical Model for Cantilevered Piezoelectric Energy Harvesters," Journal of Vibration and Acoustics 130(4), 041002 (2008).

[7] Erturk, A., and Inman, D.J., "On Mechanical Modeling of Cantilevered Piezoelectric Vibration Energy Harvesters," Journal of Intelligent Material Systems and Structures 19(11), 1311–1325 (2008).

[8] Xue, H., Hu, Y., and Wang, Q.-M., “Broadband piezoelectric energy harvesting devices using multiple bimorphs with different operating frequencies,” IEEE Transactions on Ultrasonics, Ferroelectrics and Frequency Control 55(9), 2104–2108 (2008).
[9] Adhikari, S., Friswell, M.I., and Inman, D.J., “Piezoelectric energy harvesting from broadband random vibrations,” Smart Materials and Structures 18(11), 115005 (2009).
[10] Lallart, M., Anton, S.R., and Inman, D.J., “Frequency Self-tuning Scheme for Broadband Vibration Energy Harvesting,” Journal of Intelligent Material Systems and Structures 21(9), 897–906 (2010).
[11] Stanton, S.C., McGehee, C.C., and Mann, B.P., “Nonlinear dynamics for broadband energy harvesting: Investigation of a bistable piezoelectric inertial generator,” Physica D: Nonlinear Phenomena 239(10), 640–653 (2010).
[12] Kim, I.-H., Jung, H.-J., Lee, B.M., and Jang, S.-J., “Broadband energy-harvesting using a two degree-of-freedom vibrating body,” Applied Physics Letters 98(21), 214102–214102–3 (2011).
[13] Wang, Y.-J., Chen, C.-D., Sung, C.-K., and Li, C., “Natural frequency self-tuning energy harvester using a circular Halbach array magnetic disk,” Journal of Intelligent Material Systems and Structures 23(8), 933–943 (2012).
[14] Tang, L., Yang, Y., and Soh, C.K., [Broadband Vibration Energy Harvesting Techniques] , in Adv. Energy Harvest. Methods, N. Elvin and A. Erturk, Eds., Springer New York, 17–61 (2013).
[15] Cottone, F., Gammaitoni, L., Vocca, H., Ferrari, M., and Ferrari, V., “Piezoelectric buckled beams for random vibration energy harvesting,” Smart Materials and Structures 21, 035021 (2012).
[16] Mann, B.P., “Energy criterion for potential well escapes in a bistable magnetic pendulum,” Journal of Sound and Vibration 323(3–5), 864–876 (2009).
[17] Zhu, D., Roberts, S., Tudor, J., and Beeby, S., “Closed loop frequency tuning of a vibration-based micro-generator” (2008).
[18] Ayala-Garcia, I.N., Zhu, D., Tudor, M.J., and Beeby, S.P., “A tunable kinetic energy harvester with dynamic over range protection,” Smart Materials and Structures 19(11), 115005 (2010).
[19] Yung, K.W., Landecker, P.B., and Villani, D.D., “An Analytic Solution for the Force Between Two Magnetic Dipoles,” Magnetic and Electrical Separation 9(1), 39–52 (1998).
[20] Callaghan, E.E., and Maslen, S.H., [The Magnetic Field of a Finite Solenoid] (1960).
[21] Conway, J.T., “Exact solutions for the magnetic fields of axisymmetric solenoids and current distributions,” IEEE Transactions on Magnetics 37(4), 2977–2988 (2001).
[22] Derby, N., and Olbert, S., “Cylindrical magnets and ideal solenoids,” American Journal of Physics 78(3), 229–235 (2010).